

1. Introduction

Targeted therapy, especially MWA is a highly effective method due to the good result of demolishing unhealthy target tissue [1,2]. The advantage of MWA, compare to other energy sources, for example, laser, radiofrequency, or ultrasound, is the larger ablating zone and depth effectiveness [3-9].

Several MWA improvements have been presented in recent years. The antenna designs has been presented such as cooled-shaft antenna [10]-[11], Tri-axial [12]-[13], floating sleeve [14]-[15], and slot antenna [16]-[17]. The most suitable is the slot antenna because of the comfortable size and high effective coagulating result [18]-[19]. The key factor during the ablation process, duration, input microwave power, has been studied by Keangin et al [20]. However, there remains a limitation of MWA even with recent improvement strategies, the slot antenna gave the lesion backward heating and damage the surrounding healthy tissues [21]-[23].

In this study, the porous liver model with the energy equation and momentum equation has proposed. The investigation gives the essential aspect of a fundamental understanding of heat transport within porous liver cancer. The enhance of MWA with nanoparticle has investigated and can be used as a guideline to enhance the efficacy design of MWA.

Nomenclature

k	: propagation constant (m^{-1})
C	: speed of light (m/s)
r	: dielectric radius (m)
\vec{H}	: Magnetic field (A/m)
u, w	: velocity component (m/s)
p	: pressure (Pa)
d_p	: diameter of cell tissue (m)
C_p	: specific heat capacity (J/kg °C)
\vec{E}	: Electric field (V/m)
g	: gravitation constant (m^2/s)
K	: thermal conductivity (W/(m°C))
P	: input microwave power (W)

Q	: heat source (W/m^3)
t	: time (s)
T	: temperature (°C)

Greek Symbols

ω	: angular frequency (rad/s)
ρ	: density of liver tissue (kg/m^3)
ϵ_0	: permittivity of free space (F/m)
ϵ_r	: relative permittivity (-)
σ	: electric conductivity (S/m)
μ	: permeability (H/m)
μ_r	: relative permeability
ν	: kinematics viscosity (m^2/s)
ϕ	: tissue porosity
β	: coeff. of thermal expansion (K^{-1})
κ	: permeability (m^2)

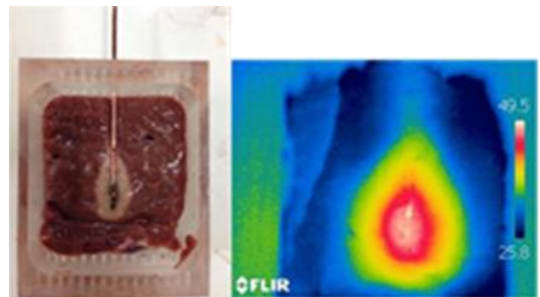
Subscripts

b	: blood/fluid phase
t	: tissue/solid phase
ext	: external
eff	: effective value
$inner$: inner
$liver$: liver
met	: metabolism

2. Problem statement

2.1 The backward heating problem

The backward heating remains a serious effect in the MWA process. It has been more serious when input power and operating durations are increased due to achieve larger lesions [20]. Fig.1 shows the backward heating problem. The photo took by our experiments performed ex-vivo with bovine liver tissue. This photo clearly shows



a tear-drop shape lesion with a long tail.

Fig.1. Demonstration of backward heating shape

To leverage the MWA performances, the two key tissue properties that are

thermal conductivity and electrical conductivity, are main factor for heat transportation in tissue. There are few studies investigate these factors, how the influence of thermal and electrical conductivity affects the blood velocity, temperature distribution in the ablation zone. Since the nanoparticle is required to elevate these two properties and investigate the result of how improving performance on temperature distribution and the ablation zone.

The influences of thermal and electrical conductivity with selected nanoparticles CNT are investigated. The newly investigated nano-hyperthermia proposed interesting ability in tumor treatment [36]. Nano-assisted cryosurgery has been proposed interesting result [37]. The magnetite (Fe_3O_4), Magnesium Oxide (MgO) and Diamond have been used to promote the thermal ablation [38]. The cylindrical carbon nanotube (CNT) has been introduced to RFA treatment and gave a good performance in the absorption of excess radiofrequency radiation [39].

In recent years, the good performance of nanoparticle assisted hyperthermia has shown positive impact [24]. Furthermore, the success of loading nanoparticle into a liver tumor is effective, to leverage the thermal and conductivity properties of liver tumor [25]-[27]. Unfortunately, only a few existing research that reports the investigation of MWA performance liver tumor therapy with nanoparticle assisted.

The performance of cancer treatment by using nanoparticle assisted hyperthermia has shown a positive impact, furthermore, the success of loading nanoparticle into the liver tumor is effective, especially the increase of thermal and electrical conductivity properties of liver tumor. Unfortunately, only a few existing studies that report the investigation of the MWA performance liver cancer treatment with nanoparticle assisted.

2.2 The precision of simulation heat transfer model

The key study in MWA performance is the precious heat transfer model. It is one of benefit tool to predict and enhance MWA treatment process. Unfortunately, there are few studies in the realistic physical model of the liver tumor. Since the complexity of the biological tissue that including with liver tissue, cell and microvascular with blood flow direction in the example, only a few studies that considered the heat transfer model with porous media theory [28]-[30].

The porous liver model with the energy equation and momentum equation has proposed. The influence of thermal and electrical conductivity in the porous liver model along with selected nanoparticles, Carbon Nanotube (CNT) has investigated. The transient momentum equation (Brinkman model extended with Darcy model) together with the transient energy equation including with electromagnetic equation, is conducted. The simulation equation and boundary conditions are calculated by using the axisymmetric FEM via COMSOL™ Multiphysics. The proposed model has been verified with previous work bio-heat models and experimental results with the same conditions. The simulation results of temperature distribution, blood velocity profile with influences of thermal and electrical conductivity factor and the selected nanoparticles CNT are presented. The investigation gives the essential aspect of a fundamental understanding of heat transport in porous liver tumors and selected nanoparticles and can be used as a guideline to enhance the efficacy of MWA for future study.

3. Simulation Methodology

3.1 Slot Microwave Antenna model

The single-slot microwave antenna has been used because of the appropriate size for insertion into the human liver. Fig. 2 has shown the antenna model structure with a slot ring of 1 mm. and position of slot far

from short circuit tip 5.5 mm. The operating frequency is 2.45 GHz. Table 1 and Fig. 2 give the antenna dimension and dielectric properties respectively [20].

3.2 Porous Liver model

The porous liver can be separate into three main parts. Which are blood vessels, cells, and interstitial space [29]-[30]. The porous liver can simplicity considered into two distinct regions. One is the vascular region (blood vessels/fluids phase). Another one is the extravascular region (tissue cell and interstitial space/solid phase). This assumes that the whole anatomical structure as a fluid-saturated porous medium through the blood infiltrates [30]. The porous liver model in this study is considered into two parts, tumor, and normal liver tissue. Fig. 2 has shown the porous liver model structure.

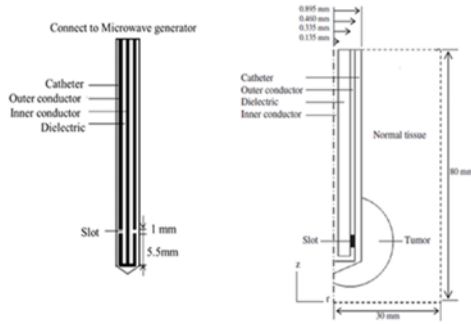


Fig. 2 Structure of the antenna and Axis symmetrical model structure [20]

Table1. The dielectric properties of a slot microwave antenna [20]

Properties	Dielectric	Catheter	Slot
Relative permittivity, ϵ_r (-)	2.03	2.1	1
Electric conductivity, σ (s/m)	0	0	0
Relative permeability, μ_r (-)	1	1	1

Table2. Properties of tissue, blood and tumor [30]-[32]

Properties	Normal tissue	Blood	Tumor
Thermal Conduct K (W/m °C)	0.497	0.45	0.57
Density ρ (kg/m ³)	1,030	1,058	1,040
Specific heat capacity C_p (J/kg. °C)	3,600	3,960	3,960
Relative Permittivity ϵ_r	43.00	58.30	48.16
Electric conductivity σ (S/m)	1.69	2.54	2.096

The tumor is a spherical shape with a diameter of 20 mm. The axis-symmetric model is used to minimizing the calculation time which maintains a good resolution. The thermal conductivity properties and dielectric properties of normal tissues and tumors have been given in Table 2 [30]-[32].

3.3 The Mathematical Model

The electromagnetic field propagation in microwave coaxial antenna and equation for heat transfer with blood flow are described as following:

3.3.1 Electromagnetic field

The equation of electric field and magnetic fields in the Transverse Electromagnetic field (TEM), which propagate in the coaxial antenna, is described in symmetrical cylindrical coordinates (2D axis r-z):

$$\vec{E} = e_r \frac{C}{r} e^{j(\omega t - kz)} \quad (1)$$

$$\vec{H} = e_\phi \frac{C}{rz} e^{j(\omega t - kz)} \quad (2)$$

$$C = \frac{\sqrt{ZP}}{\pi \cdot \ln(r_{outer}/r_{inner})} \quad (3)$$

Where

The inner dielectric radius (r_{outer}) and the outer dielectric radius (r_{inner}) have been given in Fig2., respectively [20].

In a typical MWA using a slot antenna, the thermal energy is created from the conversion of the magnetic energy when the magnetic field is radiated to the target porous liver. The Transverse Magnetic field is represented by the equation as follow:

$$\nabla \times \left[\left[\epsilon_r - \frac{j\sigma}{\omega \epsilon_0} \right]^{-1} \nabla \times \vec{H}_\phi \right] - \mu_r k_0^2 \vec{H}_\phi = 0 \quad (4)$$

Where $\epsilon_0 = 8.8542 \times 10^{-12}$ F/m [11], relative permittivity (ϵ_r) = 2.03, the electric

conductivity (σ) = 0 and relative permeability (μ_r) = 1.

Meanwhile, the boundary conditions for axis symmetry at $r = 0$, boundary condition for porous liver and slot antenna

boundary condition and electromagnetic wave propagation assumption have been obtained from literature P. Keangin et al [20]. Therefore Fig. 3 has shown the detail of the boundary condition for this study.

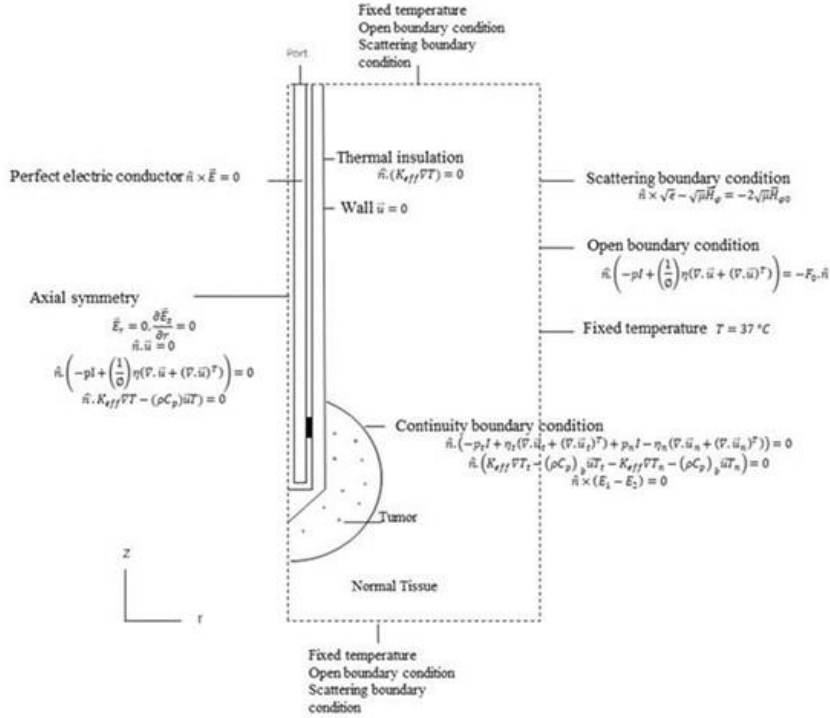


Fig. 3. Boundary conditions for this study

3.3.2 Equation for blood flow and thermal transport

To study the transient temperature distribution within the porous liver tumor and normal tissue as shown in Fig. 3, the coupled model of electromagnetic wave propagation, blood flow, and thermal transport have been analyzed. The surrounding of the porous liver is equal to 37 °C as fixed temperature whereas the surface between the antenna and the porous liver, the adiabatic boundary condition has been considered. For simplicity, several assumptions have been obtained from our previous group work [33].

3.3.3 Momentum equation

To describe the blood flow phenomenon in porous liver tumors and

normal tissue, the Brinkman model extended Darcy model is used. The equations that explained the blood flow in the porous liver are given from the continuity equation (5) and momentum equation (6) and (7) as follows [33]:

$$\frac{\partial u}{\partial r} + \frac{\partial w}{\partial z} = 0 \quad (5)$$

$$\frac{1}{\phi} \left[\frac{\partial u}{\partial t} \right] + \frac{1}{\phi^2} \left[u \frac{\partial u}{\partial r} + w \frac{\partial u}{\partial z} \right] = -\frac{1}{\rho_b} \left[\frac{\partial p}{\partial r} \right] + \frac{v}{\phi} \left[\frac{\partial^2 u}{\partial r^2} + \frac{\partial^2 u}{\partial z^2} \right] - \frac{uv}{\kappa} \quad (6)$$

$$\frac{1}{\phi} \left[\frac{\partial w}{\partial t} \right] + \frac{1}{\phi^2} \left[u \frac{\partial w}{\partial r} + w \frac{\partial w}{\partial z} \right] = -\frac{1}{\rho_b} \left[\frac{\partial p}{\partial z} \right] + \frac{v}{\phi} \left[\frac{\partial^2 w}{\partial r^2} + \frac{\partial^2 w}{\partial z^2} \right] - \frac{vw}{\kappa} + g\beta(T - T_\infty) \quad (7)$$

The tumor porosity (ϕ_{tumor}) = 0.7 and normal tissue porosity (ϕ_{n_tissue}) = 0.6. The kinematics viscosity (ν) = 3.78×10^{-7} m²/s, the coefficient of thermal expansion (β) = 11×10^{-4} K⁻¹. The permeability (κ) can be calculated by the following equation [33]:

$$\kappa = \frac{\phi^3 d_p^2}{175(1-\phi)^2} \quad (8)$$

Where diameter of cell tissue (d_p) = 1×10^{-4} m²
Energy equation

3.3.4 Energy Equation

The transient energy equation governing the thermal phenomena that created in porous liver tumor have been described as [33]:

$$(\rho C_p)_{eff} \frac{\partial T}{\partial t} + (\rho C_p)_b \left[u \frac{\partial T}{\partial r} + w \frac{\partial T}{\partial z} \right] = K_{eff} \left[\frac{\partial^2 T}{\partial r^2} + \frac{\partial^2 T}{\partial z^2} \right] + Q_{met} + Q_{ext} \quad (9)$$

$$(\rho C_p)_{eff} = (1 - \phi)(\rho C_p)_t + \phi(\rho C_p)_b \quad (10)$$

$$K_{eff} = (1 - \phi)K_t + \phi K_b \quad (11)$$

The external heat source (Q_{ext}) have been created by the electromagnetic and assumes created from tissue/solid phase only, can be expressed as [33]:

$$Q_{ext} = \frac{\sigma |\vec{E}|^2}{2} \quad (12)$$

3.3.5 The cooperated nanoparticle in MWA calculation

3.3.5.1 Thermal conductivity

The conventional Hamilton-Crosser (H-C) model have been used in calculation the cooperated thermal conductivity between nanoparticle and liver tumor tissue [34]. When the spherical nanoparticle is injected to the space between cells, the H-C model express the merged thermal conductivity and heat capacity expressed by

$$k_{effnp}(T) = k_{eff}(T) \cdot \frac{k_{np} + 2k_{eff}(T) + 2\eta(k_{eff}(T) - k_{np})}{k_{np} + 2k_{eff}(T) - \eta(k_{eff}(T) - k_{np})} \quad (13)$$

$$C_{effnp}(T) \rho_{effnp} = C_{eff}(T) \rho_{eff} (1 - \eta) + C_{np} \rho_{np} \eta \quad (14)$$

For the non-spherical structure merged nanoparticle CNT calculation. Glory et al [35] have proposed thermal conductivity for non-spherical nanoparticle as following equation:

$$k_{effnp}(T) = k_{eff}(T) \cdot \frac{k_{eff} + (n-1)k_{np} - (n-1)\eta(k_{eff}(T) - k_{np})}{k_{eff} + (n-1)k_{np} - \eta(k_{eff}(T) - k_{np})} \quad (15)$$

$$\text{where } n = \left(\frac{12L}{d}\right)^{1/3} \quad (16)$$

3.3.5.2 Electrical conductivity

In this study the electrical conductivity model of nanoparticle applied from the Maxwell's model [31]. The effective electrical conductivity when merged with nanoparticle is expressed by the following equation:

$$\sigma_{effnp}(T) = \sigma(T) \cdot \frac{3(\sigma_{np}(T) - \sigma(T))\eta}{(\sigma_{np}(T) + 2\sigma(T)) - (\sigma_{np}(T) - \sigma(T))\eta} \quad (17)$$

Since the nanoparticle has much larger conductivity than liver tumor conductivity, the equation (17) can rewrite as

$$\sigma_{effnp} = (1 + 3\eta)\sigma \quad (18)$$

3.4 Calculation Procedure

The transient phenomenon has been analyzed by using the Finite Element Method (FEM) based on COMSOLTM multiphysics. The two models of an electromagnetic equation with blood flow equation and heat transport are conducted. The temperature distribution, blood flow and ablation area that occur in the porous liver are described. The simulation starts from calculating electromagnetic wave which creates heat sources in terms of an external heat source. Then calculate the time-dependent temperature that occurs in the porous liver. The calculation process has been continuing until the target heating

time. The axisymmetric FEM model is used by using the triangular element with Lagrange quadratic shape functions. The partial differential equations with the designed boundary are conducted. The simulation has been conducted until the stability result in which the independent fine mesh is to be around 22,405.

4. Result and discussion

4.1. The model verification

The verification of the present porous liver model is compared with the simulation result of Keangin et al [20] and experimental result of Yang et al [31]. All condition has been set in same condition input microwave power 75 W with frequency 2.45 GHz with the temperature start from 8 °C and the antenna insert depth is 20 mm. The validation results have been shown in Fig. 4 for the temperature distribution in the porous liver tissue at position 4.5 mm. and 9.5 mm. away from the slot antenna. The result has shown that the porous model is better complying with experimental data than the conventional bioheat at the same approximate time range. Since the porous liver show performance with convective heat together with conduction heat, while the conventional bioheat is contained with only conduction heat mode.

The porous liver model has been studied for prediction when the key properties in the model have been changed. The influence of two keys properties, the thermal conductivity (K) and electrical conductivity (σ) on the temperature distribution in the porous liver with blood flow have been investigated. The tumor is the spherical shape with a diameter of 10 mm. A study of each parameter has been conducted to investigate the result of each factor separately. The results of changed properties when nanoparticles apply to cells also have been investigated.

4.2 The influence of thermal and electrical conductivity in porous liver with blood flow model

The influences of thermal conductivity in the porous liver with blood flow are investigated. The effective performance of MWA depends on the characteristic of the temperature profile, which determines by the key property thermal conductivity in the MWA process. The simulation of various thermal conductivity properties in the porous liver has been conducted. The heating time is 300 sec. and microwave input power (P) equal 10 watts. Fig. 5 (a) - 5 (d) has shown the temperature profile and blood flow profile within the porous liver. The various thermal conductivities of tumors have been investigated by increasing 1.5, 2.0, and 4.0 times of normal tumor condition respectively. The figure illustrates the hot spot zone, maximum temperature and blood velocity for each condition.

The effectiveness of the MWA process is to elevate the precision of the ablation area without effect the healthy tissue around the tumor. In this section, the effects of thermal property in the ablation zone in the porous liver with blood flow model have been investigated. Fig. 6 has shown the geometry of the temperature measurement point along with the arc of the tumor. The microwave input power is 10 watts. Fig. 6 (a) – 6(d) have shown the result of temperature at each measurement point within the various thermal properties. It is found that when the thermal conductivity increase, the maximum temperature will decrease. Furthermore, increase thermal conductivity such as 100 or 1000 times, results in a smaller variation of temperature in the porous liver. This is because when increase thermal conductivity will generate heat to all area rapidly with blood flow and makes temperature distribute in a uniform shape.

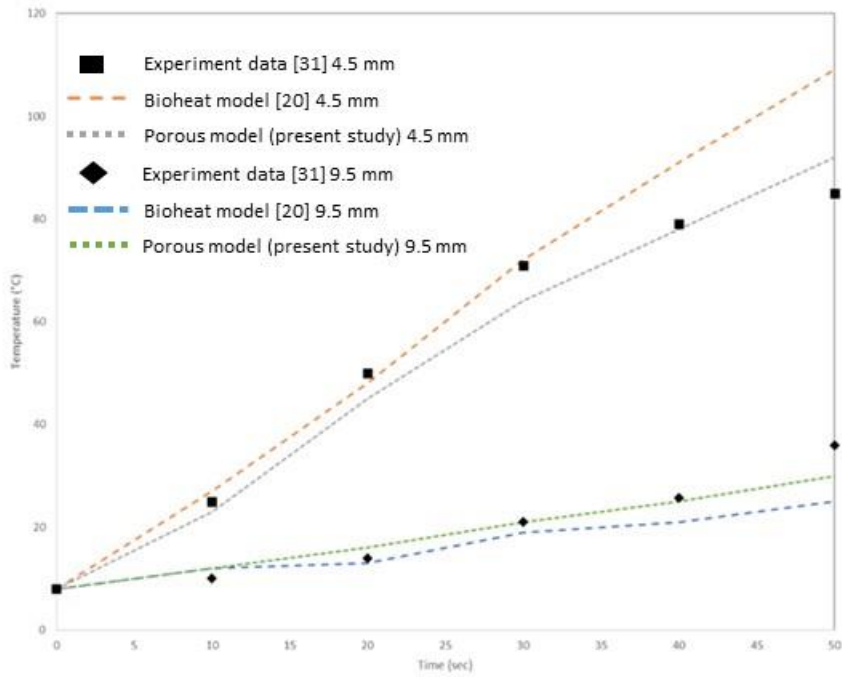


Fig. 4 The Verification result of the liver tissue temperature

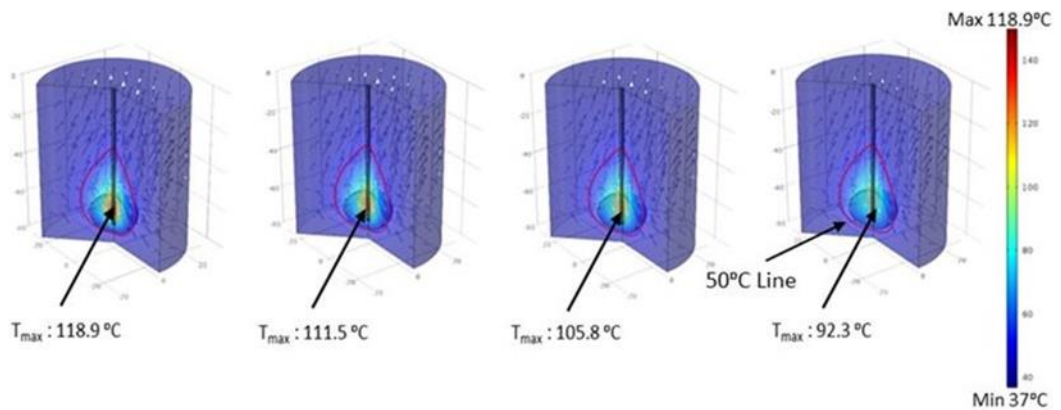


Fig. 5 The temperature pattern and blood flow vector within the porous liver at various thermal conductivity: (a) Normal tumor thermal conductivity (b) Increase 1.5 time of normal tumor condition (c) Increase 2 time of normal tumor condition (d) Increase 4 time of normal tumor condition

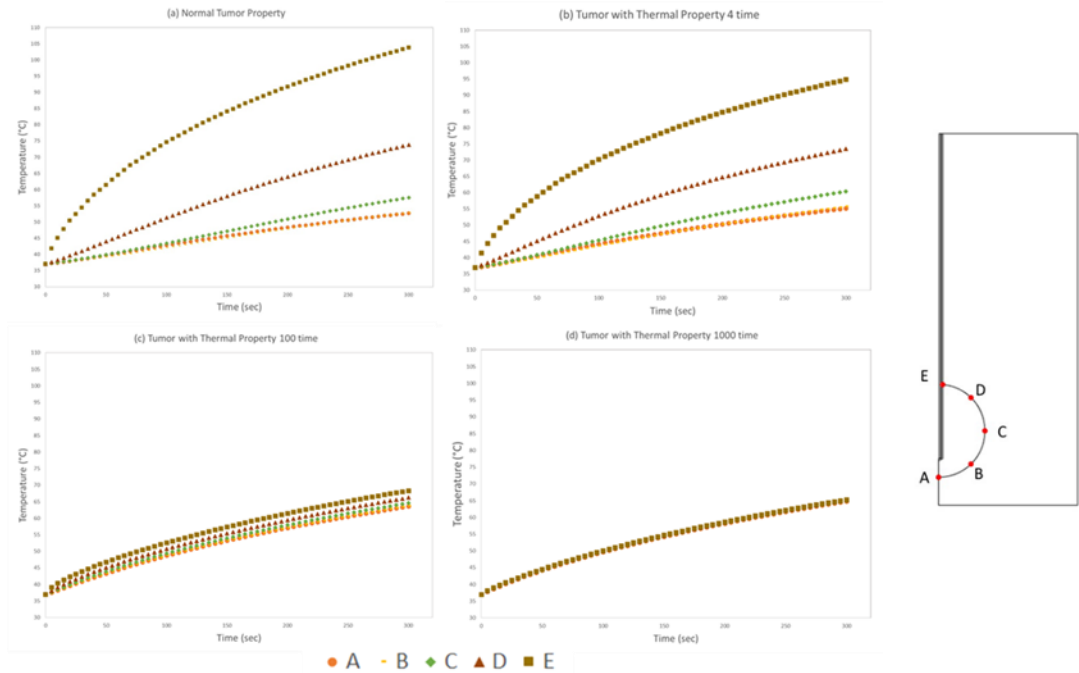


Fig. 6 The temperature distribution along the arc section of tumor at various porous liver thermal conductivity properties: (a) Normal tumor thermal conductivity (b) Increase 4 time of normal tumor condition (c) Increase 100 time of normal tumor condition (d) Increase 1000 time of normal tumor condition.

4.3 The influence of selected nanoparticles on thermal and electrical conductivity in porous liver

The nanoparticle CNT with volume fraction $\eta = 0.5$ has loaded in the equation 13 to 18, compared the result with normal tumor tissue condition. Fig. 7 shows the simulation result of the tumor temperature contour between normal tissue and loaded nanoparticle CNT with volume fraction $\eta = 0.5$. The red line is 50 °C line. Fig. 7 (a) shows the red line that did not cover the tumor 100% even though the simulation duration reaches 1000 sec. and produces a 12 mm. tail range. Fig. 7 (b) shows the red line cover tumor 100% with a simulation time 75 sec. and produce a 4 mm. tail range. Since the CNT has increased the thermal conductivity in tumor tissue, it can conclude the improved performance of MWA from these comparisons.

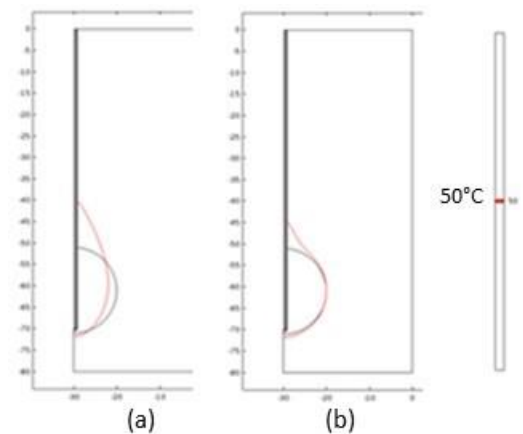


Fig. 7 Temperature contour compare between (a) Normal tissue and (b) nanoparticle CNT loaded with volume fraction $\eta = 0.5$

5. Conclusion

The Microwave ablation mathematical simulation model of heat transfer and blood

flow within the porous liver have been developed. Specifically, study the influence of thermal and electrical properties on treatment outcome and efficacy. The mathematical model has been validated with the experimental data which conducted in previous work [31]. It is found that the simulation result of the porous liver model has better result than conventional bioheat model when compared with previous experimental data [31].

Clinical treatment with MWA requires accurate control of various parameter due to the lesion creation need to create without effect to healthy tissue. To enhance the MWA process, the proposed porous liver tumor with two key properties has been investigated. The two key properties have been selected and studied in more detail for the effectiveness in the improvement MWA process. Thermal conductivity and electrical conductivity properties have been selected with the proposed porous liver model. The selected nanoparticle CNT has been included and investigate. The selected nanoparticle has been studied by using the conventional Hamilton-Crosser (H-C) thermal conductivity model [34]. The two main properties in porous liver model have been recalculated on the volume fraction. The thermal effective and electrical effective that sharing by volume fraction between selected nanoparticle and liver tumor properties, using porous liver model have been conducted. The simulation has been conducted and key finding that emerged from the result include:

(1) The proposed porous liver model gave good result than conventional bioheat when compare to the previous experimental data. It can be confirmed that the porous media theory is the most suitable theory for heat transfer in biological tissue. The proposed porous liver model with momentum equation is proved and can be

apply to the realistic model in MWA process simulation.

(2) The higher thermal conductivity is introduced to the targeted tumor tissue and found that the maximum temperature is reduced since the heat transfer and blood flow in the proposed model phenomena. Even though the temperature still higher than 50°C in ablating zone. To promote heat transfer between MWA antenna and target tumor tissue, some particle having high thermal conductivity properties such as nanoparticle needed to introduce and investigate in the future study. For the same situation, when higher electrical conductivity is introduced to the targeted tumor tissue, the maximum temperature, and heating rate are increased.

(3) The higher thermal conductivity promotes the MWA treatment by lowering the hot spot zone of tumor tissue temperature, lead to a more uniform temperature distribution within the tumor tissue. The higher thermal conductivity gives lower variation temperature in the targeted tumor. This is very usefully for elevate MWA efficiency and decrease the harmful during the MWA process.

(4) The residual tail or backward heating reduces 300 % when the higher thermal conductivity CNT loaded to targeted tumor. Since high thermal conductivity affects the temperature distribution to be uniform and absorb the temperature created from microwave power better than no particle loaded tumor tissue.

This key investigation obtains the necessary aspects of a principle knowledge of enhancing the MWA treatment process. It can be used as a guideline to study more for enhancing the MWA treatment process. Even the backward heating remains but the result has been given better results and sees more change to improve the MWA process treatment.

Acknowledgements

The authors gratefully thank you for the financial support provided by Thailand Research Fund (TRF), contact number 5980009

References

- [1] C.J. Simon, D.E. Duuy. And W.W. Mayo-smith (2005). Microwave ablation: principles and application, *Radiographics*, vol. 25, October 2005, pp. S69-S83
- [2] Alan A.S. Amad, Abimael F.D. Loula, Antonio A. Novotny (2017). A new method for topology design of electromagnetic antennas in hyperthermia therapy, *Applied Mathematical Modelling*, vol. 42, pp. 209-222
- [3] J.C. Lin, P. Bernardi, S. Pisa, M. Cavagnaro and E. PiuZZi (2008). Antenna for medical therapy and diagnostics. *Modern Antenna Handbook*, C. Balanis, Ed., Newyork: Wiley. pp. 1377-1428
- [4] A. Karampatzakis, S. Khun, G. Tsanidis, E. Neufeld, T. Samaras and Niels Kuster (2013). Heating characteristics of antenna arrays used in microwave ablation: A theoretical parametric study, *Computers in Biology and Medicine*, vol. 43 pp. 1321-1327
- [5] T.L. Wonnell, P.R. Stauffer and J.J. Langberg (1992). Evaluation of microwave and radio frequency catheter ablation in a myocardium-equivalent phantom model, *IEEE Trans. Biomed. Eng.*, vol. 39 (10) pp. 1086-1095
- [6] J.C. Lin, Y.L. Wang and R.J. Heriman (1994). Comparison of power deposition pattern produced by microwave and radio frequency cardiac ablation catheters, *Electron. Lett.*, vol. 30(12), pp. 922-923
- [7] D.L. Deardorff, C.J. Diederich and W.H. Nau (2001). Control of interstitial thermal coagulation: Comparative evaluation of microwave and ultrasound applicator, *Med. Phys.* Vol. 28(1), Jan. 2001, pp. 104-117
- [8] M.M. Attar, M. Haghpanahi, S. Amanpour and M. Mohaqeq (2014). Analysis of bioheat equation for hyperthermia cancer treatment, *Journal of mechanical Science and Tech.*, vol. 28(2), 2014, pp. 763-771
- [9] A.S. Wright, L.A. Sampson, T.F. Warner, D.M. Mahvi, and F.T. Lee Jr. (2005). Radiofrequency versus microwave ablation in a hepatic porcine model, *radiology*, vol. 236 pp. 132-139
- [10] D. Jiao, L. Qian, Y. Zhang, F. Zhang, C. Li, Z. Huang, L. Zhang, W. Zhang, P. Wu, X. Han, G. Duan and J. Han (2010). Microwave ablation treatment of liver cancer with 2,450 MHz cooled-shaft antenna: an experimental and clinical study, *Journal of Cancer Research and Clinical Oncology*, vol. 136 (10), October 2010, pp. 1507-1516
- [11] Y. Sun, Z. Cheng, L. Dong, G. Zhang, Y. Wang and P. Liang (2012). Comparison of temperature curve and ablation zone between 915 and 2450 MHz cooled shaft microwave antenna: result in ex vivo porcine livers, *European Journal of Radiology*, vol. 81 (3), March 2012, pp. 553-557
- [12] C.L. Brace, D.W. Van Der Weide, F.T. Lee Jr., P.F. Laeseke and L. Sampson (2004). Analysis and experimental validation of a triaxial antenna for microwave tumor ablation, *IEEE MTT-S International Microwave Symposium Digest*, vol. 3 (6-11), January 2004, pp. 1437-1440
- [13] C.L. Brace, P.F. Laeseke, L.A. Sampson, T.M. Frey, D.W. Van Der Wiede, F.T. Lee Jr. (2007). Microwave ablation with multiple simultaneously powered small gauge triaxial antennas: result from an in vivo swine liver model, *Radiology*, vol. 244 (1), July 2007, pp. 151-156
- [14] D. Yang, J.M. Bertram, M.C. Converse, A.P. O'Rourke, J.G. Webster, S.C. Hagness, J.A. Will and D.M. Mahvi (2006). A floating sleeve antenna yield localized hepatic microwave ablation, *IEEE transactions on Biomedical Engineering*, vol. 53 (3), March 2006, pp. 533-537
- [15] P. Prakash, G. Deng, M.C. Converse, J.G. Webster, D.M. Mahvi and M.C. Ferris (2008). Design optimization of a robust sleeve antenna for hepatic microwave ablation, *Physics in medicine and Biology*, vol. 53 (4), February (2008), pp. 1057-1069

- [16] K. Saito, H. Yoshimura, K. Ito, Y. Aoyagi and H. Horita (2004). Clinical trials of interstitial microwave hyperthermia by use coaxial-slot antenna with two slots, *IEEE Transactions on Microwave theory and techniques*, vol. 52 (8), August 2004, pp. 1987-1991
- [17] J.M. Bertram, D. Yang, M.C. Converse, J.G. Webster and D.M. Mahvi (2006). Antenna design for microwave hepatic ablation using an axisymmetric electromagnetic model, *Biomedical Engineering Online*, vol. 5, February 2006, pp. 1-9
- [18] L. Hadizafar, M.N. Azarmanesh and M. Ojaroudi (2011). Enhance bandwidth double-fed microstrip slot antenna with a pair of L-shaped slots, *Progress in Electromagnetics research*, vol. 18, November 2010, pp. 47-57
- [19] J.M. Bertram, D. Yang, M.C. converse, J.G. Webster and D.M. mahvi (2006). A review of coaxial-based interstitial antennas for hepatic microwave ablation, *critical Rev., Biomed. Eng.*, vol. 34 (3), pp. 187-213
- [20] P. Keangin, P. Rattanadecho and T. Wessapan (2011). An analysis of heat transfer in liver tissue during microwave ablation using single and double slot antenna, *International communications in Heat and Mass Transfer*, vol. 38 (6), July 2011, pp. 757- 766
- [21] P.E. Clark, R.D. Wooddruff, R.J. Zagoria and M.C. Hall (2007). Microwave ablation of renal parenchymal tumors before nephrectomy: phase I study, *American Journal of Roentgenology*, vol. 188 (5), May 2007, pp. 1212-1214
- [22] P. Phasukkit, S. Tungjitkusolmun and M. Sangworasil (2009). Finite-element analysis and in vitro experiments of placement configurations using triple antennas in microwave hepatic ablation, *IEEE Transactions on Biomedical Engineering*, vol. 56 (11), November 2009, pp. 2564-2572
- [23] M. Li, X.L. Yu, P. Liang, F. Liu, B. Dong and P. Zhou (2012). Percutaneous microwave ablation for liver cancer adjacent to the diaphragm, *International Journal of Hyperthermia*, vol. 28 (3), pp. 218-226
- [24] I. Obaidat, B. Issa, and Y. Haik (2015). Magnetic properties of magnetic nanoparticles for efficient hyperthermia, *Nanomaterial*, vol. 6 2015, pp. 63-89
- [25] D.R. Di, Z.Z. He, Z.Q. Sun, J. Liu (2012). A new nano-cryosurgical modality for tumor treatment using biodegradable MgO nanoparticles, *Nanomedicine: Nanotechnol., Biol.Med.*, vol. 8 (8), November 2012, pp. 1233-1241.
- [26] JF. Yan, J. Liu (2008). Nanocryosurgery and its mechanism for enhancing freezing efficiency of tumor tissues, *Nanomedicine: Nanotechnology, Biology Medicine*, vol. 4 (1), March 2008, pp. 79-87.
- [27] Y.L. Shao, B. Arjun, H.L. Leo and K.J. Chua (2017). Nano-assisted radiofrequency ablation of clinically extracted irregularly-shaped liver tumors, *Journal of Thermal Biology*, vol. 66, 2017, pp. 101-113
- [28] A. Nakayama and F. Kuwahara (2008). A general bioheat transfer model based on the theory of porous media, *International Journal of Heat and Mass transfer*, vol. 51 (11-12), June 2008, pp. 3190-3199
- [29] S. Mahajoob and K. Vafai (2009). Analytical characterization of heat transport through biological media incorporating hyperthermia treatment, *International Journal of Heat and Mass Transfer*, vol. 52 (5-6), February 2009, pp. 1608-1618
- [30] P.R. Stauffer, F. Rossetto, M. Prakash, D.G. Neuman and T. Lee (2003). Phantom and animal tissue for modeling the electrical properties of human liver, *International Journal of Hyperthermia*, vol. 19 (1), January-February 2003, pp. 89-101
- [31] D. Yang, M. Converse, D.M. Mahvi and J.G. Webster (2007). Expanding the bioheat equation to include tissue internal water evaporation during heating, *IEEE Transactions on Biomedical Engineering*, vol. 54 (8), August 2007, pp. 1382-1388
- [32] T. Wessapan, S. Srisawatdhisukul and P. Rattanadecho (2011). The effects of dielectric shield on specific absorption rate and heat transfer in the human body exposed to leakage microwave energy, *International Communications in Heat*

- and Mass Transfer, vol. 38 (2), February 2011, pp. 255-262
- [33] P. Rattanadecho, and P. Keangin, (2013). Numerical study of heat transfer and blood flow in two-layered porous liver tissue during microwave ablation process using single and double slot antenna, *International Journal of heat and mass Transfer*, vol. 58(1-2), March 2013, pp. 457-470
- [34] K.C. Leong, C. Yang, S.M.S Murshed (2006). A model for the thermal conductivity of nanofluids—the effect of interfacial layer. *J. Nanopart. Res.* vol 8 (2), April 2006, pp. 245–254.
- [35] J. Glory, M. Bonetti, M. Helezen, M. Mayne-L Hermite, C. Reynaud (2008). Thermal and Electrical conductivities of water-based nanofluids prepared with long multiwalled carbon nanotubes. *J. Appl. Phys.* 103 (9), February 2008, pp. 094309(1-7)
- [36] I. Obaidat, B. Issa, and Y. Haik (2015). Magnetic properties of magnetic nanoparticles for efficient hyperthermia, *Nanomaterial*, vol. 6 2015, pp. 63-89
- [37] D.R. Di, Z.Z. He, Z.Q. Sun, J. Liu (2012). A new nano-cryosurgical modality for tumor treatment using biodegradable MgO nanoparticles, *Nanomedicine: Nanotechnol., Biol.Med.*, vol. 8 (8), November 2012, pp. 1233-1241.
- [38] JF. Yan, J. Liu (2008). Nanocryosurgery and its mechanism for enhancing freezing efficiency of tumor tissues, *Nanomedicine: Nanotechnology, Biology Medicine*, vol. 4 (1), March 2008, pp. 79-87.
- [39] Y.L. Shao, B. Arjun, H.L. Leo and K.J. Chua (2017). Nano-assisted radiofrequency ablation of clinically extracted irregularly-shaped liver tumors, *Journal of Thermal Biology*, vol. 66, 2017, pp. 101-113